Interaction of the Retinal Insulin Receptor β-Subunit with the P85 Subunit of Phosphoinositide 3-Kinase†

Raju V. S. Rajala,*[,‡,§,||] Mark E. McClellan,[§,||] Michael D. Chan,[§,||] Leonidas Tsiokas,[‡] and Robert E. Anderson[‡,§,||,⊥]

Departments of Cell Biology, Ophthalmology, and Biochemistry and Molecular Biology, University of Oklahoma Health Sciences Center, and Dean A. McGee Eye Institute, Oklahoma City, Oklahoma 73104

Received October 27, 2003; Revised Manuscript Received March 15, 2004

ABSTRACT: Recently, we have shown that phosphoinositide 3-kinase (PI3K) in retina is regulated in vivo through light activation of the insulin receptor β-subunit. In this study, we have cloned the 41 kDa cytoplasmic region of the retinal insulin receptor (IRβ) and used the two-hybrid assay of protein−protein interaction in the yeast *Saccharomyces cerevisiae* to demonstrate the interaction between the p85 subunit of PI3K and the cytoplasmic region of IRβ. Under conditions where IRβ autophosphorylates, substitution of Y1322F and M1325P in IRβ resulted in the abolition of p85 binding to the IRβ, confirming that the p85 subunit of PI3K binds to Y1322. The binding site for p85 on IRβ was also confirmed in the yeast three-hybrid system. Using the C-terminal region of IRβ (amino acids 1293−1343 encompassing the YHTM motif) as bait and supplying an exogenous tyrosine kinase gene to yeast cells, we determined that the IRβ-pYTHM motif interacts with p85. We also used retinal organ cultures to demonstrate insulin activation of the insulin receptor and subsequent binding of p85, measured through GST pull-down assays with p85 fusion proteins. Further, the Y960F mutant insulin receptor, which does not bind IRS-1, is capable of bringing down PI3K activity from retina lysates. On the other hand, in response to insulin, IRS-2 is able to interact with the p85 subunit of PI3K in the retina. These results suggest that multiple signaling pathways could regulate the PI3K activity and subsequent activation of Akt in the retina.

A variety of growth factors and hormones mediate their cellular effects via interactions with cell surface receptors that possess protein kinase activity (*1*, *2*). The interaction of most of these ligands with their receptors induces tyrosine kinase activation and autophosphorylation of the receptor, resulting in physical association of the receptors with several cytoplasmic substrates having SH2 domains (*3*, *4*). Phosphoinositide 3-kinase (PI3K)[1] has been identified through its ability to associate with cellular protein kinases, including numerous growth factor receptors and oncogene products (*3*, *4*).

PI3K activity increases in response to PDGF binding to its receptor, in large part because the class Ia p85/p110 complex is translocated from the cytosol to the plasma membrane, by the direct binding of the p85 SH2 domain to tyrosine-phosphorylated sites on the receptor (*5*, *6*). Insulin receptor activation stimulates intrinsic tyrosine kinase activity that leads to autophosphorylation. However, unlike the EGF and PDGF receptors, the phosphorylated insulin receptor does not usually directly associate with SH2 proteins (*7*). Rather, the activated insulin receptor usually phosphorylates IRS-1, a principal substrate of the insulin receptor, on multiple tyrosine residues, which in turn recognizes and binds to the SH2 domain of various signal transduction proteins (*8*). With few exceptions (*9*), PI3K is activated when phosphorylated IRS-1 binds to the SH2 domain in its p85α regulatory subunit, which establishes a direct molecular connection between circulating insulin and this cellular enzyme (*10*).

Cells of bovine and rat retina contain high-affinity receptors for insulin (*11*−*14*). Rodrigues et al. (*15*) found the insulin receptor in photoreceptor and neuronal cell bodies, with lower immunoreactivity in rod outer segments (ROS). We have also demonstrated the presence of insulin receptors in both outer and inner segments of isolated bovine rods (*16*). Bovine ROS also contain a class Ia PI3K that is more active in light-adapted retinas in vitro (*17*) and can be activated by tyrosine phosphorylation of IRβ in vitro (*18*). We have recently shown that PI3K in ROS is associated with light-activated (tyrosine-phosphorylated) IRβ in vivo (*16*, *19*).

It is interesting to note from our previous study that the association of PI3K with tyrosine-phosphorylated IRβ appeared to be independent of IRS-1 (*18*), even though there

† This work was supported by grants from the National Institutes of Health (Grants EY00871, EY04149, EY12190, DK59599, and RR17703), Research to Prevent Blindness Inc., New York, NY, The Foundation Fighting Blindness, Baltimore, MD, and Presbyterian Health Foundation, Oklahoma City, OK. R.V.S.R. is a recipient of a Career Development Award from Research to Prevent Blindness.

* To whom correspondence should be addressed. Telephone: 405-271-8255. Fax: 405-271-8128. E-mail: raju-rajala@ouhsc.edu.

‡ Department of Cell Biology, University of Oklahoma Health Sciences Center.

§ Department of Ophthalmology, University of Oklahoma Health Sciences Center.

|| Dean A. McGee Eye Institute.

⊥ Department of Biochemistry & Molecular Biology, University of Oklahoma Health Sciences Center.

[1] Abbreviations: PI3K, phosphoinositide 3-kinase; GST, glutathione *S*-transferase; IRβ, insulin receptor β subunit; PAGE, polyacrylamide gel electrophoresis; PCR, polymerase chain reaction; ROS, rod outer segments; IPs, immunoprecipitates; PI-4,5-P_2, phosphatidylinositol 4,5-bisphosphate; PI-3,4,5-P_3, phosphatidylinositol 3,4,5-trisphosphate; PDGF, platelet-derived growth factor; SDM, site-directed mutagenesis.

10.1021/bi035913v CCC: $27.50
Published on Web 04/21/2004

is widespread expression of IRS-1 throughout the retina (*20*). It has been shown previously that the direct interaction of the insulin receptor with PI3K represents a minor alternative pathway, compared to the tyrosyl-phosphorylated IRS-1, in the activation of PI3K (*9*). Consistent with this suggestion is the observation that the juxamembrane mutant of the insulin receptor shows diminished IRS-1 phosphorylation and PI3K activation, despite normal phosphorylation of the C-terminus (*21*, *22*). On the other hand, inactivation of the IRS-1 gene in mice by homologous recombination did not result in any dramatic phenotype (*23*, *24*), suggesting the possible existence of alternative signaling pathways. The direct activation of receptor-associated PI3K is important in subcellular fractions such as endosomes, which have been shown to contain tyrosine-phosphorylated insulin receptor (*25*) and PI3K (*26*). Further, it has recently been shown that, in gestational diabetes mellitus, PI3K activity was associated with IRβ, not IRS-1 (*27*).

The association of PI3K with tyrosine-phosphorylated IRβ in retina, independent of IRS-1, led us to speculate that retinal IRβ could be different from the previously reported insulin receptors or that a different regulatory mechanism could control the insulin receptor mediated functions. To further explore these possibilities, we have cloned the 41 kDa cytoplasmic domain of the retinal insulin receptor and used the two-hybrid assay of protein−protein interaction in the yeast *Saccharomyces cerevisiae* to study the interaction between p85, IRS-1, IRS-2, and IRβ. Retinal organ cultures were also developed to study the above interactions in response to insulin. In this study, we have demonstrated the mechanism of activation of retinal PI3K and subsequent activation of Akt.

EXPERIMENTAL PROCEDURES

Materials. Polyclonal anti-IRβ, anti-IGF1-R, anti-IRS-1, anti-IRS-2, anti-IRS-3, anti-IRS-4, anti-IRS-1 agarose conjugate, anti-IRS-2 agarose conjugate, and monoclonal anti-PY-99 antibodies were from Santa Cruz Biotechnology (Santa Cruz, CA). Polyclonal anti-p85 antibody was obtained from Upstate, Inc. (Lake Placid, NY). Anti-glutathione *S*-transferase (GST) antibody and glutathione−Sepharose 4B matrix were obtained from Amersham Biosciences Corp. (Piscataway, NJ). [γ-^{32}P]ATP was from New England Nuclear (Boston, MA). Echelon Research Laboratories, Inc. (Salt Lake City, UT), provided D-myophosphatidylinositol 4,5-bisphosphate (PI-4,5-P_2). Anti-Akt, anti-pAkt (Ser 473), Akt kinase assay kit, and HA-tag antibodies were obtained from Cell Signaling Technology, Inc. (Beverly, MA). HA epitope tag agarose conjugate was obtained from Novus Biologicals (Littleton, CO). Human insulin R (rDNA origin) was obtained from Eli Lilly & Co. (Indianapolis, IN). All other reagents were of analytical grade from Sigma (St. Louis, MO).

Plasmid Constructs. The retinal insulin receptor cytoplamic domain (accession number AY566293) was obtained by PCR of reverse-transcribed retina RNA using a 5′- and 3′-oligonucleotides designed on the basis of rat liver insulin receptor (sense, ccgtcgacgaattcaggaagaggcagccagat; antisense, cgtcgacttaggaagggttcgacctcggcgagg) (*28*). The cDNA encoding the cytoplasmic domain of the rat insulin receptor (amino acids 941−1343) was cloned into the pBTM116 yeast two-hybrid vector. The full-length cDNA encoding p85 (p85 FL) was a generous gift from Dr. Deborah H. Anderson (University of Saskatchewan, Saskatoon, Canada). The full-length p85 cDNA was excised from the pGEX-2T vector as a *Bam*HI/*Eco*RI fragment and subcloned into the pAD-GAL4-2.1 yeast vector carrying the GAL4 activation domain. The cDNA fragments encoding the N-SH2 domain of p85 and its respective SH2 mutant (R358A) were amplified from the full-length p85 cDNA and subcloned into the pVP16 activation domain. The cDNA encoding full-length Grb10 (amino acids 4−536) (*29*) was a generous gift from Dr. Thomas Gustafson (Metabolex, CA). The Grb10-IR SH2 (amino acids 413−536) domain was amplified from the human brain cDNA library (Clontech) employing the primers (sense) cgggatccacgggaggatctccagggaggaa and (antisense) cggaattctcataaggccactcggatgcag and cloned into the pVP16 vector. All constructs were verified by DNA sequencing before cloning them into yeast hybrid vectors.

The cDNA fragments encoding amino acids 144−316 from IRS-1 (sense, cgcggatccgcgacttgagctatgacacgggc; antisense, ccggaattctggttcccacccaccatact) and amino acids 191−350 (sense, cgcggatccgctaccgcgaggtgtggcag; antisense, ccggaattctgctgggggggtggccgc) and 591−786 (sense, cgcggatccgcctagatgaatacactctc; antisense, ccggaattcgaggccttcactgcctcc) from IRS-2 were amplified from first strand cDNA reverse transcribed from rat (IRS-1) and mouse (IRS-2) retinal RNA. The PCR products were verified by DNA sequencing, digested with *Bam*HI and *Eco*RI, and cloned into plasmid pACT2 (ATCC, Manassas, VA), encoding the GAL4 activation domain.

Yeast Two-Hybrid Assay. Yeast transformations were performed by the lithium acetate method as described (*30*). Briefly, 0.5 μg of each plasmid (LexA DNA-binding domain or GAL4 transactivation domain fusion) was used to simultaneously transform the L40 yeast strain [*MAT*α *HIS3*Δ200 *trp1-901 leu2-3,112 ade2 LYS2*::*(lexop)4-HIS3 URA3*::*(lexAop)8-lacZ GAL4*] that harbors both His and LacZ reporters under the control of LexA binding sites (*31*). Transformants were plated on media lacking tryptophan and leucine or tryptophan, leucine, and histidine plus 5 mM aminotriazole. Growth on media lacking tryptophan and leucine secured the presence of both plasmids independently of protein−protein interactions and further eliminated the possibility of false negatives. Selection on media lacking tryptophan, leucine, and histidine plus 5 mM aminotriazole was used to detect potential interactions. Cells surviving on these plates were further screened for LacZ phenotype by filter assay (*32*). Lifted colonies were scored for LacZ phenotypes by detection of blue color in the presence of 5-bromo-4-chloro-3-indolyl β-D-galactosidase after incubation at room temperature for 4 h. Positive control constructs such as TRPCI and PKD2 (*33*) vectors were transformed in L40, whereas PVA3-1 [murine p53 (amino acids 72−390) in pAS2.1; pTD1-1 (SV40 large T antigen (amino acids 84−708)] was transformed in Y-190 [MA*Ta*, *ura3-52*, *his3-200*, *lys2-801*, *ade2-101*, *trp1-901*, *leu2-2,112 gal4*Δ, *gal80*Δ, *cyh*^{r}*2*, *LYS2::GAL1*$_{UAS}$-*HIS3*$_{TATA}$-*HIS3*, *URA3::GAL1*$_{UAS}$-*GAL1*$_{TATA}$-*lacZ*) yeast strain.

Interaction Mating. Interaction mating experiments were carried out as described (*34*). L40 yeasts were mated with yeast strain AMR-70 [*MAT*α *HIS3*Δ200 *lys2 trp1leu2 URA3::(lexop)8-lacZ GAL4*]. Following overnight mating on

YPD medium, reaction contents were spread on plates lacking tryptophan and leucine or tryptophan, leucine, and histidine for selection of diploids. All interactions were tested in at least three independent transformations.

Filter and Liquid β-Galactosidase Assays. For filter β-galactosidase assays, yeast patches were replica lifted onto Whatman 40 filter paper and grown for 24 h. After being frozen in liquid nitrogen, these filters were laid over a Whatman 3 filter soaked in Z buffer [50 mM sodium phosphate buffer (pH 7.0), 10 mM KCl, 1 mM $MgSO_4$] with 0.5% β-mercaptoethanol and 0.2 mg/mL 5-bromo-4-chloro-3-indolyl β-D-galactopyronoside (X-gal) (Gibco BRL, Life Technologies). After 2−6 h, the reaction was stopped by incubating the filters in 1 M Na_2CO_3 and drying them at 30 °C in an incubator.

For liquid β-galactosidase assays (*35*), yeast was grown overnight on appropriate selective media. Cells were pelleted and resuspended in 5 mL of Z buffer, and the OD_{600} was recorded. Eight hundred microliters (either diluted or straight) was transferred to 1.5 mL Eppendorf tubes. Using a Pasteur pipet, 1 drop (∼50 μL) of 0.1% SDS and 2 drops of chloroform were added to each tube, which was vortexed for 15 s and allowed to equilibrate at 30 °C for 15 min. Then 160 μL of 2-nitrophenyl β-D-galactopyronoside (ONPG, 4 mg/mL in H_2O) was added, the solution was vortexed for 10 s, and the tubes were incubated at 30 °C. The tubes were removed after about 15−20 min (empirically determined by color), and the color was quenched by adding 400 μL of 1 M Na_2CO_3. The cell debris was removed by centrifugation, and the OD of the supernatant was measured at 420 and 550 nm. Results are expressed as Miller units: one unit of β-galactosidase was defined as $1000[OD_{420} - (1.75 \times OD_{550})]/[(\text{time}) \times (\text{vol}) \times OD_{600}]$.

Modified Yeast Two-Hybrid System. These vectors was kindly provided by Drs. Larry Rohrschneider [pBTM116/PDGF (*36*)] and Jonathan Cooper [pBTM116/cSRC (*37*)] from Fred Hutchinson Cancer Research Center, Seattle, WA. The modified vector (pBTM116/PDGF) has a tyrosine kinase expression cassette containing the ADHI promoter and the cytoplasmic domain of βPDGF receptor cDNA; the terminator has been inserted into a *Pvu*II site of the pBTM116 vector (*36*). Tyrosines 1009 and 1021 have been substituted with phenylalanine to eliminate the binding of proteins having SH2 domains (*36*). The carboxyl-terminal tail of IRβ (amino acids 1293−1343) was amplified from rat retina cDNA employing primers specific to this region (sense, 5′-ggatcctctcactgtcagagagaagaggct; antisense, 3′-gaattcttaggaagggttcgacctcggcga). All PCR products were sequenced, and the insert was cloned into the pBMT116 and pBTM116/PDGF vector.

Retinal Organ Cultures. Retinas were removed from Sprague-Dawley albino rats that were born and raised in dim cyclic light (5 lux; 12 h on; 12 h off). Retinas were incubated at 37 °C in DMEM medium (Gibco BRL) in the presence and absence of insulin for 0−60 min. At indicated times, retinas were snap frozen in liquid nitrogen and stored at −80 °C until analysis. In some experiments, the PI3K inhibitor LY294002 was added to the culture medium, and the retinas were incubated for 30−60 min prior to the addition of insulin.

3T3-L1 adiopocytes were kindly provided by Dr. Ann Louise Olson, Department of Biochemistry, OUHSC. 3T3-L1 adipocytes were prepared according to the method described (*38*). 3T3-L1 adipocytes were used as control since these cells exhibit insulin-induced activation of PI3K through the involvement of IRS-1 and IRS-2 (*38*).

Immunoprecipitation (IP). Retinal lysates were solubilized for 30 min at 4 °C in a lysis buffer containing 1% Triton X-100, 137 mM NaCl, 20 mM Tris-HCl (pH 8.0), 10% glycerol, 1 mM EGTA, 1 mM $MgCl_2$, 1 mM PMSF, 0.2 mM Na_3VO_4, 10 μg/mL leupeptin, and 1 μg/mL aprotinin. Insoluble material was removed by centrifugation at 17000*g* for 20 min, and the solubilized proteins were precleared by incubation with 40 μL of protein A−Sepharose for 1 h at 4 °C with mixing. The supernatant was incubated with either anti-PY (4 μg) or anti-IRβ (4 μg) or anti-IRS-1 (2 μg) or anti-IRS-2 (2 μg) antibodies overnight at 4 °C and, subsequently, with 40 μL of protein A−Sepharose for 2 h at 4 °C. Following centrifugation at 14000 rpm for 1 min, immune complexes were washed twice with modified solubilization buffer (1% Triton X-100 was reduced to 0.1% and glycerol was removed) and once with buffer B [50 mM Tris-HCl (pH 7.4), 100 mM NaCl, and 2 mM $MgCl_2$]. Immunoprecipitates were either assayed for PI3K activity or subjected to immunoblot analysis.

SDS−PAGE and Western Blot Analysis. Proteins were resolved by 10% SDS−PAGE and transferred onto nitrocellulose membranes, and the blots were washed two times for 10 min with TTBS [20 mM Tris-HCl (pH 7.4), 100 mM NaCl, and 0.1% Tween-20] and blocked with either 10% bovine serum albumin or nonfat dry milk powder (Bio-Rad) in TTBS overnight at 4 °C. Blots were then incubated with anti-IRβ (1:250), anti-PY (1:1000), p85 (1:4000), anti-IRS-1 (1:1000), anti-GST (1:5000) antibodies overnight at 4 °C. Following primary antibody incubations, immunoblots were incubated with HRP-linked secondary antibodies (either anti-rabbit, anti-mouse, or anti-goat) and developed by ECL according to the manufacturer's instructions.

Phosphoinositide 3-Kinase Assay. Enzyme assays were carried out as previously described (*39*). Briefly, assays were performed directly on immunoprecipitates in 50 μL of the reaction mixture containing 0.2 mg/mL PI-4,5-P_2, 50 μM ATP, 0.2 μCi of [γ-^{32}P]ATP, 5 mM $MgCl_2$, and 10 mM HEPES buffer (pH 7.5). The reactions were carried out for 15 min at room temperature and stopped by the addition of 100 μL of 1 N HCl followed by 200 μL of chloroform/methanol (1/1 v/v). Lipids were extracted and resolved on oxalate-coated TLC plates (silica gel 60) with a solvent system of 2-propanol/2 M acetic acid (65/35 v/v). The plates were coated in 1% (w/v) potassium oxalate in 50% (v/v) methanol and then baked in an oven at 100 °C for 1 h prior to use. TLC plates were exposed to X-ray film overnight at −70 °C, and radioactive lipids were scraped and quantified by liquid scintillation counting.

GST-p85 Fusion Proteins and Pull-Down Experiments. Cloning of GST-p85 N-SH2 and GST-p85 N-SH2 (R358A) was described previously (*18*). The amino acids of bovine p85α present in each fusion protein are p85 full length (1−724) and N-SH2 (314−446), based on the sequence published by Otsu et al. (*3*). The N-SH2 (amino acids 547−659) and C-SH2 (amino acids 663−752) domains of PLCγ1 from bovine brain were cloned by reverse transcription polymerase chain reaction. The sequence of each clone was verified by DNA sequencing. All inductions yielded proteins of the expected size as judged by Coomassie staining. Pull-

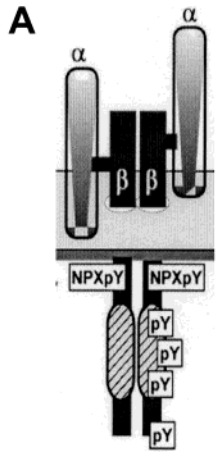

RKRQPDGPMGPL**Y**ASSNPE**Y**LSASDVFPSSVYVPDEWEVPREKITLLRELG
QGSFGMVYEGNAKDIIKGEVETRVAVKTVNESASLRERIEFLNEASVMKGFT
CHHVVRLLGVVSKGQPTLVVMELMAHGDLKSHLRSLRPDAENNPGRPPPTL
QEMIQMTAEIADGMAYLNAKKFVHRDLAARNCMVAHDFTVKIGDFGMTRDI
YETD**YY**RKGGKGLLPVRWMSPESLKDGVFTASSDMWSFGVVLWEITSLAE
QP**Y**QGLSNEQVLKFVMDGG**Y**LDPPDNCPERLTDLMRMCWQFNPKMRPTF
LEIVNLLKDDLHPSFPEVSFFYSEENKAPESEELEMEFEDMENVPLDRSSHC
QREEAGCREGGSSLSIKRTYDEHIP**Y**THMNGGKKNGRVLTSPRSNPS

FIGURE 1: Retinal insulin receptor cytoplasmic domain (IRβ). Schematic representation of the insulin receptor (A) and amino acid sequence of the rat retinal insulin receptor cytoplasmic domain (B). IRβ was cloned from rat retina total RNA by reverse transcription polymerase chain reaction employing rat liver cDNA primers as described in Experimental Procedures. Autophosphorylation sites for tyrosine (**Y**) residues are underlined. The Genbank accession number for the cytoplasmic domain of IRβ is AY566293.

down experiments were carried out as described (*40*) using 5 μg of GST fusion proteins that had been adsorbed onto the glutathione−Sepharose 4B matrix. Retina lysates and ROS from insulin treatments were incubated with GST/GST fusion proteins at 4 °C for 1.5 h with continuous stirring. The Sepharose beads were washed three times in 500 μL of HNTG buffer [20 mM HEPES (pH 7.5), 150 mM NaCl, 0.1% Triton X-100, and 10% glycerol] and centrifuged at 5000 rpm for 30−60 s at 4 °C. Bound proteins were eluted by boiling in 2 × SDS sample buffer 5 min prior to 10% SDS−PAGE. After SDS−PAGE, the gels were subjected to Western blot analysis with anti-IRβ, anti-IGF1-R, and anti-IRS-1 antibodies.

Site-Directed Mutagenesis. Site-directed mutagenesis was carried out with the Quickchange site-directed mutagenesis kit (Stratagene Inc., LaJolla, CA) using a PTC 100 programmable thermal controller (MJ Research, Inc., Watertown, MA). The reaction mixture contained SDM buffer [200 mM Tris-HCl (pH 8.8), 100 mM KCl, 100 mM $(NH_4)_2SO_4$, 20 mM $MgSO_4$, 1% Triton X-100, 1 mg/mL nuclease-free bovine serum albumin, 1 mM deoxynucleotide mix (dATP, dCTP, dTTP, and dGTP), 50 ng of vector, and 125 ng of sense and antisense primers with mutations] in a total volume of 50 μL, followed by the addition of 2.5 units of *pfu* DNA polymerase. The primers used in the site-directed mutagenesis are as follows: Y960F (sense, tcaaacccagagttcctcagtgccagt; anti-sense, actggcactgaggaactctgggtttg), Y1146F (sense, atgacgagagacatcttcgagacagattac; antisense, gtaatctgtctcgaagatgtctctcgtcat), Y1150F (sense, atctacgagacagatttctatcggaaaggg; antisense, ccctttccgatagaaatctgtctcgtagat), Y1151F (sense, atctacgagacagattactttcggaaaggg; antisense, ccctttccgaaagtaatctgtctcgtagat), Y1316F (sense, agcatcaaacggacctttgatgaacacatc; antisense, gatgtgttcatcaaaggtccgtttgatgct), Y1322F (sense, gaacacatccccttcacccacatfaacggg; antisense, cccgttcatgtgggtgaaggggatgtgttc), M1325P (sense, ccctacaccccacccgaacgggggcaagaag; antisense, cttcttgcccccgttcgggtgggtgtaggg), K1018A (sense, gagacccgtgttgcggtggcgacggtcaatgag; antisense, ctcattgaccgtcgccaccgcaacacg), and p85 N-SH2 (R358A) (sense, acctttttggtagcagacgcatctactaaa; antisense, tttagtagatgcgtctgctaccaaaaaggt). Mutations of R358A and R649A (*18*) were created individually or in combination in full-length p85 cDNA. The extension parameters of SDM were as follows: initial denaturation at 95 °C for 30 s, followed by 16 cycles at 95 °C for 30 s, at 55 °C for 1 min, and at 68 °C for 12 min (2 min/kb of plasmid length). Following temperature cycling, the reaction was placed on ice for 2 min, after which 10 units of DPN 1 restriction enzyme were added, mixed, and incubated at 37 °C for 60 min. Transformation was carried out by adding 1 μL of the DPN 1 treated reaction mixture to Epicurean XL-blue supercompetent cells at 4 °C for 30 min, followed by 60 min at 37 °C with shaking. The reaction mixture was then placed on LB/Amp (100 μg/mL) plates. The cDNAs of all mutants were sequenced after PCR, and the only mutations observed were those intentionally introduced to create each desired mutation. After sequencing, IRβ mutants were excised from the TOPO vector as *Eco*RI/*Sal*I and cloned into the pBTM116 vector. Plasmid DNA was prepared from IRβ mutants and used for yeast two-hybrid assays.

Construction and Phosphorylation of IRS-1$^{656-762}$. A fragment of the IRS-1 (*41*) corresponding to R657-L760 was PCR amplified to contain *Bam*HI and *Eco*RI restriction sites using *pfu* polymerase. The primers were (sense strand) 5′-gccggatccagagtggaccccaatggc and (antisense strand) 5′-gaggaattcctagaggactggcttgtcc. The resulting fragment was subcloned into pGEX-2TK (Amersham Pharamacia Biotech), and the integrity of the construct was verified by sequencing. This fragment contains potential phosphorylations sites, which are the in vivo binding sites for p85 following tyrosine phosphorylation (*42*). To verify whether retinal p85 can interact with this fragment, we phosphorylated this fusion protein in *Escherichia coli* by coexpressing a tyrosine kinase VSRC under the control of different replicons. The phosphorylated and nonphosphorylated (−VSRC) GST-IRS-1 $^{656-762}$ fusion proteins were purified employing glutathione−Sepharose beads.

RESULTS

Two-Hybrid Assay of Interactions between p85 and IRβ. We cloned the 41 kDa cytoplasmic region of the retinal insulin receptor (IRβ) (Figure 1) and used the two-hybrid assay of the protein−protein interaction in the yeast *S. cerevisiae* to study the interaction between the p85 subunit of PI3K and the cytoplasmic region of the retinal insulin receptor. The cloned cytoplasmic domain is similar to the

previously reported insulin receptor cytoplasmic region with more than 95% homology (*43*). Expression of the cytoplasmic domain of IRβ in the absence of α subunits has been shown to be constitutively active, and the protein autophosphorylates (*44*). The p85 subunit formed a specific complex with the cytoplasmic domain of the insulin receptor when both are expressed as hybrid proteins in yeast cells (Figure 2). This interaction is strictly dependent upon receptor tyrosine kinase activity, since p85 shows no interaction with a kinase-inactive receptor hybrid containing a mutated ATP-binding site (K1018A) (Figure 2A). The lysine residue is highly conserved in several oncogene products and growth factor receptors (*43*, *45*) and lies in a region homologous to the known ATP-binding site of several proteins (*46*). The same mutant receptor expressed in Chinese hamster ovary cells has been shown to lack tyrosine kinase activity in vitro and to be defective in mediating several biological responses to insulin (*47*, *48*). McClain et al. (*49*) have also shown that, in Rat1 fibroblasts, this kinase-defective mutant receptor does not undergo endocytosis and does not mediate ligand internalization or degradation. Further, in our study, the mutant insulin receptor (K1018A) can be expressed in yeast and is readily detectable with specific antibody, suggesting that this mutation does not cause the protein to be unstable (Figure 9). This observation is further substantiated from the experiments done on retinal organ cultures (Figures 4 and 5) showing that p85 binds to IRβ only under insulin-stimulated conditions, attesting to the role of phosphorylation in the binding between p85 and IRβ. These data suggest that the interaction between p85 and receptor is direct and provide evidence that tyrosine kinase activity is necessary. Substitution of arginine with alanine (R358A) in the N-SH2 domain of p85 prevented any interaction with wild-type IRβ (Figure 2A), further supporting the specific interaction between the N-SH2 domain and phosphorylated tyrosine residues in the insulin receptor.

Retinal IRβ interacted with IRS-1 (amino acids 144−316), full-length Grb10, and Grb10-SH2 domains (Figure 2A). In yeast two-hybrid assays, IRS-1 (*44*) and Grb10 (*29*) have been shown to interact with the insulin receptor. To confirm the interactions, we used two positive controls, which are the interactions between TRPCI and PDK2 and between p53 (PVA3-1) and large T-antigen (PTD1-1) (Figure 2B).

The p85 subunit of PI3K and the insulin receptor were expressed individually in haploid strains, which were subsequently assayed for LacZ activity after interaction mating (diploids). There was a positive read-out phenotype in the wild type and absence of LacZ expression when the K1018A mutant insulin receptor and p85 N-SH2 subunit of PI3K were used (Figure 2C). Measurement of LacZ enzyme activity supported these results (Figure 2D). These interaction-mating experiments further confirm the direct association between p85 and IRβ in diploid strains.

Tyrosine Phosphorylation Sites on IRβ. The phosphorylation site prediction program (*50*) (http://www.cbs.dtu/services/NetPhos/) was used to indicate which tyrosine residues within the retinal IRβ sequence are most likely to be phosphorylated. This program examines the sequence context of each tyrosine residue (i.e., the four residues before and after each tyrosine) and assigns an output score between 0 and 1. Scores above 0.5 are possible phosphorylation sites, and the higher the score, the more likely a particular site

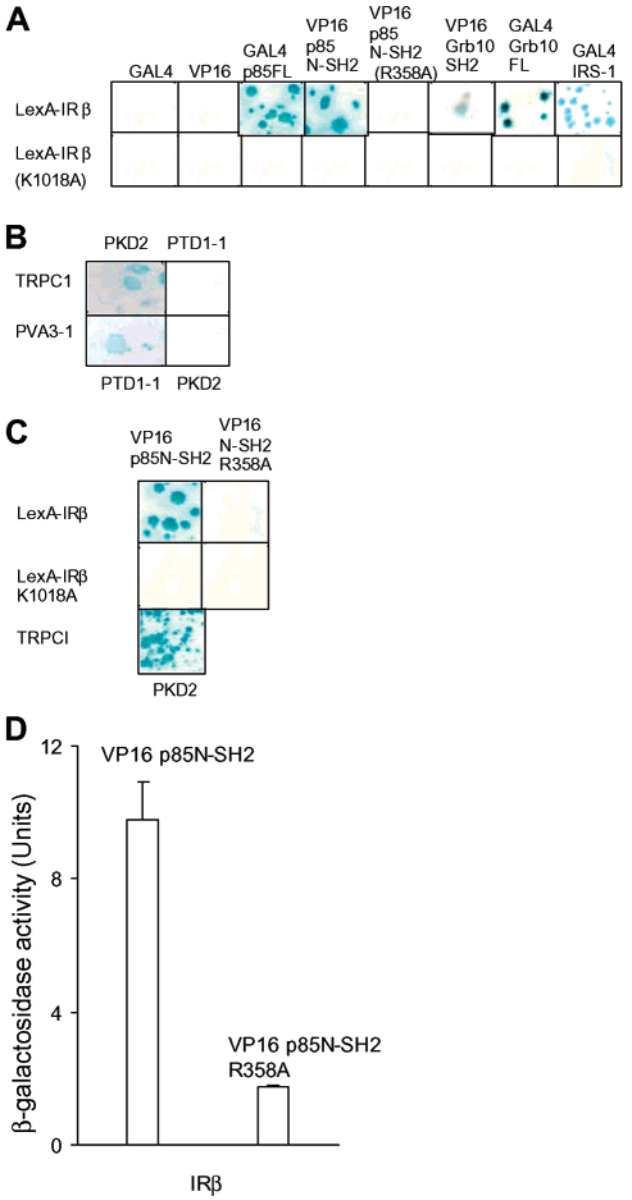

FIGURE 2: Interactions of p85, Grb10, and IRS-1 with IRβ in the yeast two-hybrid assay. The entire cytoplasmic domain of the retinal insulin receptor and K1018A mutant retinal insulin receptor was fused to the LexA DNA-binding domain (DBD). Interaction of these hybrid proteins would be expected to drive expression of the *lexAop-lacZ* reporter gene. Transformants were assayed for β-galactosidase assay by colony color as described in Experimental Procedures (A). LexA-TRPCI/GAL4-PKD2, GAL4-murine p53 (PVA3-1), and GAL4-SV40 large T antigen (PTD1-1) were cotransformed into L40 and Y-190 yeast strains and used as positive controls. Negative controls include LexA-TRPCI/GAL4-SV40 large T antigen and murine p53/GAL4-PKD2. Transformants were assayed for β-galactosidase assay by colony color (B). Tyrosine phosphorylation and SH2-dependent binding of the retinal insulin receptor and the p85 subunit of PI3K were studied through interacting mating. Yeast diploids were obtained by mating L40 and transformed with the entire cytoplasmic domain (wild type or K1018A mutant) of retinal insulin receptor (LexA DNA-binding domain) and with AMR-70 transformed with constructs carrying VP16-p85 N-SH2 or its mutant (R358A). For positive control we used TRPCI (L40) and PKD2 (AMR-70) and carried out the interaction mating experiments as described above. Transformants were assayed for β-galactosidase assay by colony color (C). Yeast cells were grown overnight, and transformants were isolated on selected media. Transformants were assayed for β-galactosidase activity by the solution assay as described in Experimental Procedures (D).

Table 1: Prediction of Tyrosine Phosphorylation on Tyrosine Residues in the Retinal Insulin Receptor Cytoplasmic Domain

Tyr position	sequence[a]	score[b]	prediction
953	MGPL**Y**ASSN	0.898	Y
960	SNPE**Y**LSAS	0.979	Y
972	PSSVYVPDE	0.254	
999	FGMVYEGNA	0.151	
1110	DGMAYLNAK	0.272	
1146	TRDI**Y**ETDY	0.755	Y
1150	YETD**Y**YRKG	0.983	Y
1151	ETDY**Y**RKGG	0.833	Y
1198	AEQP**Y**QGLS	0.547	Y
1215	MDGG**Y**LDPP	0.966	Y
1266	VSFFYSEEN	0.062	
1316	IKRTYDEHI	0.072	
1322	EHIP**Y**THMN	0.633	Y

[a] The amino acid sequence surrounding the Tyr (Y). [b] Phosphorylation scores were calculated on the basis of the phosphorylation site prediction program (*50*) (http://www.cbs.dtu.dlk/serverces/Net.Phos/). Scores above 0.5 are deemed to be possible phosphorylation sites, and the higher the score, the more likely a particular site will be phosphorylated.

Table 2: Site-Directed Mutagenesis of Selected Lysine/Tyrosine/Methionine Residues in the Retinal Insulin Receptor Cytoplasmic Domain[a]

Lys/Tyr/Met mutation	β-galactosidase activity[b]	
	p85	IRS-1
WT	+++	+++
K1018A	−	−
Y960F	+++	−
Y1316F	+++	+++
Y1322F	−	+++
M1325P	−	+++

[a] Yeast two-hybrid assays were carried out as described in Experimental Procedures. [b] Colony color was assayed in three independent transformations: +++, strong interaction; −, no interaction.

will be phosphorylated. This approach predicts phosphorylation sites in independent sequences with a sensitivity of 69−96% (*50*, *51*). Our analysis indicated that, of the 13 tyrosine residues in the IRβ, five residues are unlikely phosphorylation sites, with scores less than 0.3 (Table 1). The most likely tyrosine phosphorylation sites are 953, 960, 1146, 1150, 1151, 1198, 1215, and 1322 (Table 1).

p85 Binding to Tyrosine 1322 on IRβ. Substitution of Y1322F and M1325P in IRβ abolished p85 binding to the phosphorylated insulin receptor (Table 2) and confirmed that the p85 subunit of PI3K binds to Y1322 in phosphorylated IRβ (*52*). Methionine has been shown to be invariably found in the +3 position of known PI3K binding sites (*53*, *53*). This residue has been selected from the degenerate peptide library by both p85 SH2 domains (*54*). In addition, substitution of Y960F and Y1316F did not affect the binding of p85 to IRβ, whereas substitution of Y960F abolished binding of IRS-1 to IRβ (Table 2). Since p85 binds to Y1322 on IRβ, it seems unlikely that other tyrosine residues may contribute to the p85 binding. Hence, we did not study the interaction of p85 with other mutant tyrosine residues in IRβ except Y960 and Y1316.

Effect of Coexpression of the Insulin Receptor C-Tail, p85 Proteins, and Tyrosine Kinase in Yeast. To demonstrate that Y1332 is the binding site of the p85 N-SH2 domain, we cloned the cytoplasmic tail of IRβ (amino acids 1293−1343 encompassing Y1322) into the modified pBTM116 vector.

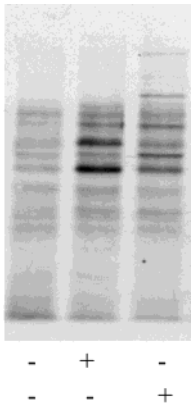

FIGURE 3: Expression and phosphorylation of proteins in yeast. *S. cerevisiae* L40 stain was transformed with either the LexA vector or modified LexA vector carrying either the cSrc or PDGF-β receptor. Yeast proteins were prepared by employing the Fast Protein Red kit (Q Bio gene) and subjected to Western blot analysis with anti-PY antibody.

This peptide does not contain the autophosphorylation domain. The interaction between SH2 and phosphotyrosine requires tyrosine kinase activity. Since yeast *S. cerevisiae* may not express tyrosine kinases with appropriate specificity, the two-hybrid system was modified such that the bait plasmid encoding the LexA-IRβ (1293−1343) fusion protein also coexpressed a tyrosine kinase. The source of tyrosine kinase in this vector was the cytoplasmic domain of the βPDGF receptor (*36*). To preclude the SH2 domain binding to the PDGF-β receptor, a mutant containing tyrosine to phenylalanine was substituted at 1009 and 1021 in the PDGF-β receptor (*36*). Thus, this tyrosine kinase could potentially phosphorylate either the LexA-IRβ or a cDNA clone expressed as VP16 or GAL4 fusion proteins but should not compete with targets for binding to IRβ. To test whether the tyrosine kinase induced phosphorylation in yeast, lysates of yeast cells expressing either the LexA vector or LexA vector together with the PDGF-β receptor or cSrc were immunoblotted and probed with an anti-PY antibody. In the absence of tyrosine kinase, there were very low levels of phosphorylation, while the expression of the tyrosine kinase resulted in tyrosine phosphorylation of several yeast proteins (Figure 3).

Interaction between various p85 proteins and IRβ containing Y1322 (amino acids 1293−1343) in the presence and absence of tyrosine kinase activity (PDGF-β) is presented in Table 3. p85 FL and IRβ interacted only in the presence of tyrosine kinase, demonstrating the necessity of tyrosine phosphorylation. However, IRS-1 failed to interact with pY1322, indicating that Y1322 is the binding site for p85, but not for IRS-1, on IRβ.

Effect of Length of the Protein on Interactions. Wild-type IRβ containing the kinase domain (amino acids 941−1343) interacted with p85 FL (Figure 2), as well as with p85 FL containing individual mutations in either N-SH2 (R358A) or C-SH2 (R649A) (Table 2). Individually expressed N-SH2 and C-SH2 domains of p85 also interacted with IRβ. However, neither domain, when mutated and expressed as the truncated protein, interacts with IRβ. This suggests that binding by either N-SH2 or C-SH2 domains is sufficient to interact with phosphorylated IRβ to produce the observed LacZ activation in the yeast two-hybrid assays.

Table 3: Analysis of the Yeast Three-Hybrid System[a]

interaction	β-galactosidase activity colony color[b]
LexA	−
LexA-IRβ/p85FL	−
LexA-IRβ/IRS-1	−
LexA/VP16	−
LexA/p85FL	−
LexA/PDGF	−
LexA-PDGF	−
LexA-IRβ/p85FL/PDGF	++
LexA-IRβ/IRS-1/PDGF	−

[a] Yeast three-hybrid assays were carried out as described in Experimental Procedures. [b] Colony color was assayed in three independent transformations: +++, strong interaction; ++, moderate interaction; −, no interaction.

Table 4: Effect of Length of Protein on Interactions[a]

DNA-binding domain fusion	activation domain fusion	colony color[b]
IRβ 941-1343	p85FL 1-724	
IRβ 1293-1343	p85 (NSH2) 314-446	
	p85 (CSH2) 663-752	
two-hybrid assay		
LexA IRβ (941−1343)	p85FL (1−724)	+++
LexA IRβ (941−1343)	p85FL (1−724) R358A	+++
LexA IRβ (941−1343)	p85FL (1−724) R649A	+++
LexA IRβ (941−1343)	p85FL (1−724) R358, 649A	−
LexA IRβ (941−1343)	p85 N (SH2) (314−446)	+++
LexA IRβ (941−1343)	p85 N (SH2) (314−446) R358A	-
LexA IRβ (941−1343)	p85 C (SH2) (663−752)	+++
LexA IRβ (941−1343)	p85 C (SH2) (663−752) R649A	−
three-hybrid assay		
LexA IRβ (1293−1343)	p85FL (1−724)	++
LexA IRβ (1293−1343)	p85FL (1−724) R358A	++
LexA IRβ (1293−1343)	p85FL (1−724) R649A	++
LexA IRβ (1293−1343)	p85FL (1−724) R358, 649A	−
LexA IRβ (1293−1343)	p85 N (SH2) (314−446)	−
LexA IRβ (1293−1343)	p85 N (SH2) (314−446) R358A	−
LexA IRβ (1293−1343)	p85 C (SH2) (663−752)	−
LexA IRβ (1293−1343)	p85 C (SH2) (663−752) R649A	−

[a] Yeast two- and three-hybrid assays were carried out as described in Experimental Procedures. Numbers in parentheses indicate the length of the protein expressed (amino acids). [b] Colony color was assayed in three independent transformations: +++, strong interaction; ++, moderate interaction; −, no interaction.

Coexpression of the C-terminal tail of IRβ (amino acids 1293−1343) with a tyrosine kinase led to an interaction with p85 FL (amino acids 1−724) (Table 4). p85 FL containing individual mutations in either N-SH2 (R358A) or C-SH2 (R649A) still interacted with IRβ. However, simultaneous substitution of alanine for arginine at positions 358 and 649 in p85 FL completely abolished this interaction. It is interesting to note that neither N-SH2 nor C-SH2 domains of p85, as well as their respective mutants, interacted with IRβ when expressed as small domains and tested individually. These experiments indicate that IRβ containing amino acids 941−1343 (41 kDa) interacts with p85 FL as well as with N-SH2 and C-SH2 domains of p85, whereas IRβ containing amino acids 1293−1343 (5.5 kDa) interacts with

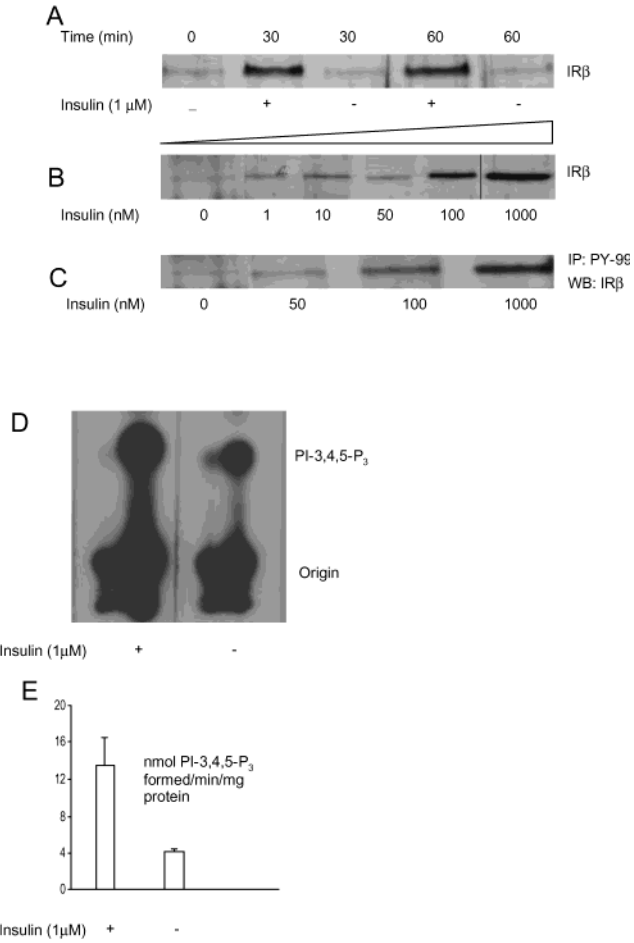

FIGURE 4: Time- and concentration-dependent activation of insulin receptor in retinal cultures. Retinas were cultured in DMEM in the presence and absence of insulin at different times (A) and at various concentrations of insulin (B). After insulin stimulation, retinal lysates were immunoprecipitated with PY-99 antibody and immunoblotted with anti-IRβ antibody (C). TLC autoradiogram of PI3K activity measured in anti-IRβ IPs of insulin and unstimulated retinas using PI-4,5-P_2 and [γ-^{32}P]ATP as substrates (D). The radioactive spots of PI-3,4,5-P_3 were scraped from the TLC plate and counted (E). Data are the mean ± SD ($n = 3$).

p85 FL but not with its expressed N-SH2 and C-SH2 domains. These results suggest that, for efficient binding between the phosphorylated tyrosine residue in IRβ and the SH2 domains in p85, one protein should be longer in length (either IRβ or p85) than the other.

Activation of the Insulin Receptor by Insulin in Organ Cultures. Addition of insulin to the DMEM incubation medium resulted in activation of the insulin receptor, measured by receptor phosphorylation in GST pull-down assays. Under phosphorylation conditions (presence of insulin), the p85 N-SH2 domain of PI3K could pull down IRβ as detected on the Western blots probed with anti-IRβ antibody. These results further confirm our observations of the endogenous interactions between IRβ and p85 (*18*). More IRβ was recovered in GST pull downs at longer incubation times (Figure 4A). Likewise, more IRβ was recovered as the concentration of insulin was increased from 1 to 1000 nM (Figure 4B). Receptor phosphorylation was confirmed in anti-PY immunoprecipitates of insulin-treated and untreated retina lysates by probing with anti-IRβ antibody. Increased IRβ signal was present in Western blots of anti-PY-99 IPs, demonstrating a dose-dependent phosphorylation

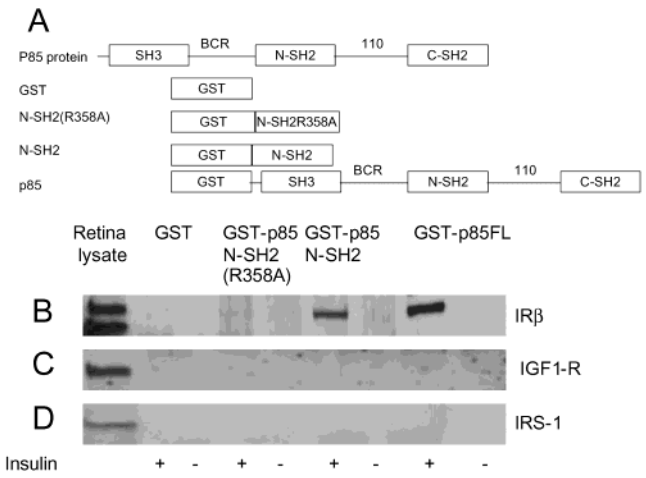

FIGURE 5: GST pull-down experiments. Rat retinas were dissected and incubated at 37 °C in DMEM medium in the presence and absence of insulin. After incubation, the retinas were lysed and subjected to GST pull-down assay (125 μg) with GST, GST-p85N-SH2 (R358A), GST-p85N-SH2, or GST-p85 full-length fusion proteins (A), followed by Western blot analysis of the bound proteins with anti-IRβ antibody (B). The blot was stripped and reprobed with either anti-IGF1-R (C) or anti-IRS-1 (D) antibodies.

of IRβ in response to insulin (Figure 4C). Higher PI3K activities were observed in the anti-IRβ IPs of insulin-stimulated retinas (Figure 4D,E). Cell culture studies in other laboratories have used concentrations of insulin between 10 and 1000 nM (*9*, *13*, *55*). In our study, we used 1000 nM insulin in most of the experiments unless otherwise indicated.

Insulin-Dependent Binding of p85. To characterize the binding of p85 to the phosphorylated insulin receptor, we used GST fusion proteins of either full length or the N-SH2 domain of the regulatory subunit of PI3K. Insulin-treated and untreated retinas were lysed and subjected to GST pull-down assays with the GST fusion proteins, as listed in Figure 5A. GST and the GST-p85 N-SH2 (R358A) mutant protein failed to pull down IRβ from either insulin-stimulated or unstimulated rat retinas, while the p85 N-SH2 domain or p85 full-length protein pulled down IRβ from insulin-stimulated rat retinas (Figure 5B). This blot was stripped and individually reprobed with anti-IGF1-R and anti-IRS-1 antibodies. The GST-p85 wild-type fusion proteins do not bring down either IGF1-R (Figure 5C) or IRS-1 (Figure 5D) proteins, although both proteins are expressed in retina. These results demonstrate that insulin does not activate IGF1-R in the retina and that the interaction of the insulin receptor with the p85 subunit of PI3K is independent of IRS-1. This is not the case in other cell types, where the interaction between the insulin receptor and PI3K is mediated through IRS-1 (*42*).

Insulin-Dependent Binding of PLCγ1. To determine if IRβ can interact with proteins other than p85 that contain SH2 domains, retinas were incubated in the presence and absence of insulin, followed by GST-pull-down assays of the retinal homogenates with N-SH2 and C-SH2 domains of PLCγ1. Insulin-stimulated IRβ interacted specifically with the C-SH2 domain of PLCγ1 but not with the N-SH2 domain (Figure 6). These results suggest that IRβ may also regulate the light activation of PLCγ1 in the retina, which has been reported previously (*56*).

Binding of the p85 Subunit of PI3K to the Phosphorylated Fragment of IRS-1 in Vitro. To verify whether retinal p85

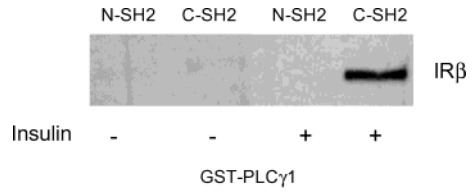

FIGURE 6: GST pull-down experiments. Insulin-stimulated and unstimulated retinas were lysed and subjected to GST pull-down assays (125 μg of protein) with GST fusion proteins of the N- and C-SH2 domains of PLCγ1. Western blot analysis of the bound proteins was probed with anti-IRβ antibody.

can interact with IRS-1, we constructed a GST fusion protein encompassing the binding sites of p85 (Figure 7A), as described in Experimental Procedures. The GST vector and GST vector containing the p85 binding sites of IRS-1 were either expressed or coexpressed in *E. coli* along with a tyrosine kinase (VSRC). Bacterial cultures were subjected to SDS−PAGE followed by Western blotting analysis with anti-Src (Figure 7B), anti-PY (Figure 7C), or anti-GST (Figure 7D) antibodies. The presence of VSRC expression in the bacterial cultures indicates that the tyrosine kinase is stable in *E. coli* (Figure 7B). To determine whether the fusion protein is phosphorylated by tyrosine kinase, an identical blot probed with anti-PY antibody (Figure 7C) showed phosphorylation of GST-IRS-$1^{656-762}$ only when it was coexpressed with VSRC. None of the proteins in the *E. coli* lysates was phosphorylated by VSRC. Autophosphorylation of VSRC occurred in *E. coli* expressing either GST or GST fusion proteins (Figure 7C). The same blot shown in Figure 7B was reprobed with anti-GST antibody without stripping and showed the presence of GST and GST-IRS-$1^{656-762}$ in the appropriate lysates (Figure 7D). The results presented in Figure 8C,D demonstrate the unique property of our *E. coli* expression system that allows coexpression of several proteins (VSRC and GST or GST-IRS-1) in the same cell.

The phosphorylated and nonphosphorylated GST-IRS-$1^{656-762}$ fusion proteins were purified by employing glutathione−Sepharose beads. Phosphorylated (three individual clones) and nonphosphorylated (two individual clones) fusion proteins were subjected to SDS−PAGE followed by Western blotting analysis with anti-PY (Figure 7E) and anti-GST antibody (Figure 7F). The results indicate that the tyrosine phosphorylation is stable in the fusion proteins, and the GST blot indicates the amount of fusion in each experiment. Phosphorylated and nonphosphorylated GST-IRS-$1^{656-762}$ fusion proteins were incubated with lysates from insulin-stimulated and nonstimulated retinas and subjected to GST pull-down assays. The results indicate that p85 was bound to phosphorylated GST-IRS-$1^{656-762}$ under both experimental conditions but not to nonphosphorylated GST-IRS-$1^{656-762}$ (Figure 7G). To determine whether the phosphorylation of GST-IRS-$1^{656-762}$ is stable during GST pull downs, we reprobed the blot with anti-PY antibody. The results indicate phosphorylation on the fusion protein (Figure 7H), although the amount of phosphorylated GST fusion protein was reduced (Figure 7I), suggesting that the phosphorylated fusion protein might be targeted to some degradation. This also occurs when we coexpress either GST or GST-IRS-$1^{656-762}$ alone with VSRC; the expression of these proteins is significantly reduced compared to their expression pattern in the absence of VSRC (Figure 7D). These experiments demonstrate that phosphorylated IRS-1 is able to bind p85.

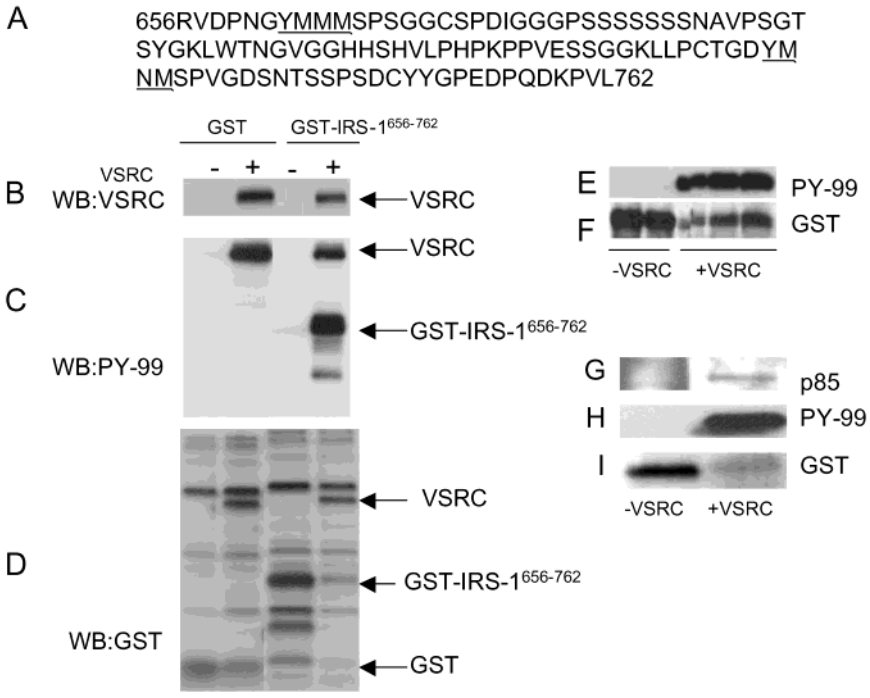

FIGURE 7: Expression of phosphorylated GST-IRS-1$^{656-762}$ and its binding to the p85 subunit of PI3K. The region between amino acids 656 and 762 was PCR-amplified from IRS-1 cDNA (A) and subcloned into pGEX-2TK vector. GST and GST-IRS-1$^{656-762}$ constructs were either expressed alone or coexpressed along with a tyrosine kinase VSRC. p85 binding sites on IRS-1 are underlined (A). Bacterial cultures were subjected to SDS−PAGE followed by Western blotting analysis with anti-Src (B), anti-PY (C), and anti-GST (D) antibodies. Phosphorylated and nonphosphorylated GST-IRS-1$^{656-762}$ fusion proteins were purified employing glutathione−Sepharose beads, and the purified proteins were Western blotted with anti-PY (E) and anti-GST (F) antibodies. Rat retina lysates were incubated with either phosphorylated or nonphosphorylated GST-IRS-1$^{656-762}$ fusion proteins and subjected to GST pull-down assays. The bound proteins were washed, boiled, and subjected to SDS−PAGE followed by Western blot analysis with anti-p85 (G), anti-PY (H), and anti-GST (I) antibodies.

In addition, we have also observed a decrease in the phosphorylation signal on the fusion proteins, when we incubated retina lystates during pull-down assays (data not shown). This decrease could be due to the presence of an active tyrosine phosphatase in the retina/rod outer segments, as has been reported previously (*57*).

Effect of Insulin on IRS-1 Phosphorylation. Retinas were incubated with and without insulin, followed by either GST pull-down assay with the GST-p85 N-SH2 domain of p85 or immunoprecipitation with the anti-IRS-1 antibody. Increased IRβ was found in insulin-stimulated p85 pull-down assays (Figure 8C). IRS-1 IPs probed with anti-IRS-1 antibody indicated similar amounts of IRS-1 in insulin- and non-insulin-stimulated conditions (Figure 8A), but IRS-1 was not tyrosine phosphorylated in either condition as determined with anti-PY antibody (Figure 8B). This experiment clearly demonstrates that, in these retinal explants, IRS-1 is not tyrosine phosphorylated by the insulin receptor. Total Akt levels examined with anti-Akt antibody showed similar amounts of Akt protein in insulin-stimulated and non-insulin-stimulated conditions (Figure 8F). However, Ser 473 phospho-Akt levels were higher in insulin-stimulated retinas compared to non-insulin-stimulated retinas (Figure 8E). The phosphorylation of Akt was reduced when the retinas were incubated with PI3K inhibitor LY294002 prior to the addition of insulin (Figure 8G), although total Akt levels were similar in both conditions (Figure 8H). These results suggest that insulin-stimulated Akt activation is mediated through PI3K, and this activation appears to be independent of IRS-1 involvement.

Endogenous interactions between p85 and IRβ have been reported previously (*18*). We have also observed that the endogenous p85 interacts with IGF1-R in ATP-treated bovine retinal rod outer segments, whereas endogenous interaction between p85 and IRS-1 is much weaker/absent compared to the interactions between IRβ and p85 (data not shown).

Interaction of Retinal IRβ with IRS-1 and IRS-2. 3T3-L1 adipocytes and rat retinas were stimulated in culture with and without insulin, and lysates were immunoprecipitated with either anti-IRS-1 or anti-IRS-2 agarose conjugate followed by immunoblotting with the anti-p85 antibody. The IRS-1 interacted with the p85 subunit of PI3K in 3T3-L1 adipocytes, and the increase in p85 binding was quite evident under insulin-stimulating conditions (Figure 9A). Retinal IRS-1 failed to interact with the p85 subunit of PI 3K in both insulin- and non-insulin-stimulated conditions (Figure 9A). To rule out the possibility that IRS-2 or another IRS family member (IRS-3 and IRS-4) might be involved in the insulin-induced activation of PI3K, we examined the expression of IRS-2, IRS-3, and IRS-4 in rat retinal homogenates. We observed the expression of IRS-2 in the retina in addition to IRS-1; however, IRS-3 and IRS-4 expression was absent (data not shown). We also observed the presence of IRS-1 and IRS-2 messages in mouse and rat retina by semiquantitative RT-PCR (data not shown).

In this study, we cloned the cDNA fragments encoding the retinal IRS-2 PTB domain (amino acids 191−350) and a region between amino acids 591−786 in IRS-2, which were expressed as in-frame fusion to the GAL4 activation domain and subjected to yeast two-hybrid assay with retinal IRβ. The retinal IRS-1 PTB domain (amino acids 144−316) was also expressed as GAL4-fusion and used in yeast two-hybrid assays. The PTB domain of both IRS-1 and IRS2 (data not shown) and a region between amino acids 591−786 in IRS-2

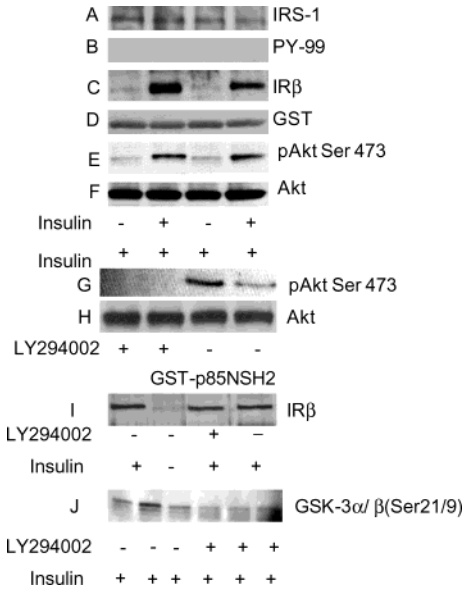

FIGURE 8: Insulin-induced activation of Akt. Rat retinas were dissected and incubated in DMEM medium with or without insulin (100 nM). After incubation, the retinas were lysed, and 150 μg of protein was subjected to GST pull-down assay with the GST-p85N-SH2 domain followed by Western blot analysis with anti-IRβ antibody (C) and anti-GST antibody (D) to examine the amount of fusion protein. Retina lysates (150 μg) were subjected to immunoprecipitation with anti-IRS-1 antibody and subjected to Western blot analysis with anti-IRS-1 (A) and anti-PY antibody (B). Twenty micrograms of retina lysate was subjected Western blot analysis with anti-Akt (F) and anti-phospho-Akt (Ser 473) (E) antibodies. Rat retinas were preincubated in DMEM medium with or without the PI3K inhibitor LY294002 (50 μM) for 60 min prior to insulin treatment. Twenty micrograms of retina lysate was subjected to Western blot analysis with anti-phospho-Akt (Ser 473) (G) and total Akt (H) antibodies. In similar experiments, retinas were lysed and subjected to GST pull-down assay (125 μg) with GST-p85 N-SH2, followed by Western blot analysis of the bound proteins with anti-IRβ antibody (I). Retina lysates (125 μg) were also immunoprecipitated with anti-Akt antibody, and the IP was used to measure the phosphorylation of GSK-3α/β (Ser 21/9). Phosphorylation products were run on SDS−PAGE followed by Western blot analysis with anti-phospho-GSK-3 antibody (J). All experiments were run at least in triplicate.

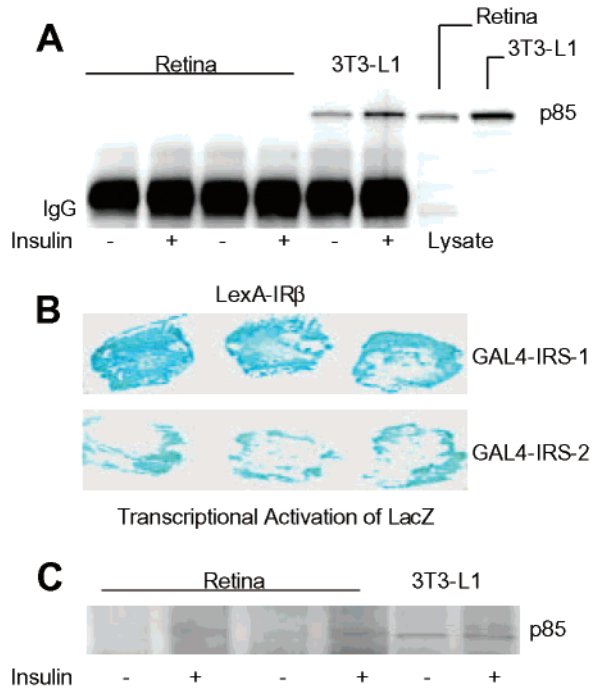

FIGURE 9: Interaction of IRS-1 and IRS-2 with retinal IRβ. 3T3-L1 adipocytes and rat retinas were stimulated in culture with and without insulin. After insulin stimulation, retinal lysates were immunoprecipitated with anti-IRS-1 agarose conjugate and immunoblotted with anti-p85 antibody. Rat retina and 3T3-L1 adipocyte lysates were used as control. The heavy chain of IgG indicates an equal amount of antibody in all the lanes (A). The L40 yeast strain was transformed with either LexA-IRβ and IRS-1 (amino acids 144−316) or LexA-IRβ and IRS-2 (amino acids 591−786), and the yeast two-hybrid assay was carried out as described in Experimental Procedures. Three independent transformants were assayed for β-galactosidase activity for colony color (B). 3T3-L1 adipocytes and rat retinas were stimulated in culture with and without insulin. After insulin stimulation, retinal lysates were immunoprecipitated with anti-IRS-2 agarose conjugate and immunoblotted with anti-p85 antibody (C).

were found to interact with retinal IRβ in yeast two-hybrid assays (Figure 9B).

Rat retinas were stimulated with insulin at various time points followed by immunoprecipitation of retinal lysates with anti-IRS-2 antibody and immunoblotting with anti-PY antibody. IRS-2 was phosphorylated within 2 min after insulin stimulation (data not shown).

To examine whether IRS-2 is involved in the activation of retinal PI3K, we immunoprecipitated the lysates from insulin- and non-insulin-stimulated rat retinas and 3T3-L1 adipocytes with anti-IRS-2 antibody. The immunoprecipitates were subjected to immunoblot analysis with anti-p85 antibody, and the results indicate that IRS-2 is able to bring down p85 from both rat retina and 3T3-L1 adipocytes. These results suggest that IRS-2 could be involved in the activation of PI3K in the retina (Figure 9C).

Role of PI3K in Insulin-Stimulated Phosphorylation of GSK-3α/β (Ser 21/9) by Akt. Retinas were preincubated in culture medium with or without the PI3K inhibitor LY294002 for 60 min prior to the addition of insulin. Retina lysates were prepared, subjected to GST pull-down assay with the GST-p85 N-SH2 domain of PI3K, and examined for IRβ in the pull downs. Increased binding of IRβ was present in GST pull downs of insulin-stimulated retinas compared to non-insulin-stimulated retinas (Figure 8I). It is interesting to note that LY294002 did not affect the binding of the p85 subunit of PI3K to the phosphorylated insulin receptor (Figure 8I). Insulin-induced phosphorylation of GSK-3α/β (Ser 21/9) by *Akt* was reduced in retinas pretreated with LY294002 (Figure 8J). These results suggest that insulin mediated its effects via the insulin receptor in the activation of *Akt* in these retinal cultures.

Binding of the p85 Subunit of PI3K to the Insulin Receptor with the Y960F Mutation. It is known that IRS-1 binds to the NPXY motif on the insulin receptor cytoplasmic domain (*58*) and that mutation in Y960F in the insulin receptor abolishes the binding of IRS-1 (*21*). To demonstrate the direct binding of PI3K to the insulin receptor in the absence of IRS-1, we expressed the insulin receptor with a Y960F mutation, as well as with a Y1322F mutation, which does not interact with the p85 subunit of PI3K, and a K1018A mutation, which results in a kinase-dead insulin receptor. We introduced a hemagglutinin (YPYDYPDYA) tag at the amino-terminal end of the insulin receptor to facilitate the pull-down experiments. Insulin receptor mutant proteins were expressed in yeast *S. cerevisiae*, and the proteins were isolated using Y-PER extraction reagent (Pierce, Rockford,

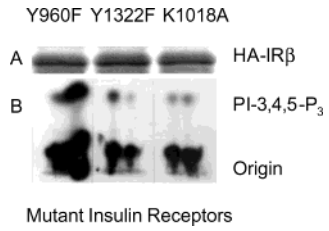

FIGURE 10: PI3K activity associated with insulin receptor containing a Y960F mutation. The cytoplasmic domains of the insulin receptor containing mutations in either Y960F, Y1322F, or K1018A were expressed in *S. cerevisiae*. Yeast proteins were prepared and Western blotted with anti-HA tag antibody (A). Yeast lysates containing the mutant insulin receptors were immunoprecipitated with anti-HA agarose conjugate, and the bound proteins were washed and incubated overnight with rat retina lysates (200 μg). The bound proteins were washed, and the PI3K activity was measured using PI-4,5-P_2 and [γ-^{32}P]ATP as substrates (B).

IL) containing 100 mM DTT and protease inhibitors according to the manufacturer's instructions. Yeast lysates containing these mutant proteins Western blotted with an anti-HA tag antibody indicated equal expression of these mutant proteins (Figure 10A). Mutant insulin receptors were isolated from yeast lysates by employing a HA agarose conjugate, and the immunoprecipitates were incubated with non-insulin-stimulated rat retina lysates. Bound proteins were washed and subjected to PI3K assay. PI3K activity was associated with the Y960F mutant insulin receptor to a greater extent than with the Y1322F and K1018A mutant receptors as shown on the TLC autoradiogram (Figure 10B). These results indicate that the Y960F mutant insulin receptor is capable of interacting with the p85 subunit of PI3K independent of IRS-1 and that IRS-2 could be involved in the activation of PI3K.

IRS-1 and IRS-2 have NH_2-terminal phosphotyrosine binding domains (PTB), which bind to the phosphorylated NPXY motif (Y960) in IRβ (*59*). Substitution of Y960F completely abolished the binding mediated through the PTB binding domain of IRS-1 (Table 2) and IRS-2 (data not shown). In addition to the PTB domain, IRS-2 interacts with IRβ via a second domain comprising amino acids 591−786, which does not require NPXY but does require Y1146, Y1150, and Y1151 in the catalytic domain of IRβ (*59*). Mutation in these residues abolished the binding of IRS-2 to IRβ (Figure 11). We homogenized retinas in the presence of 4 mM EDTA to block endogenous/exogenous tyrosine kinase activities. Under these conditions, incubation of the Y960F mutant insulin receptor should not catalyze the phosphorylation of endogenous IRS-2. However, the Y960F mutant insulin receptor still was able to interact with endogenous p85 (Figure 10). Thus, in the absence of IRS-2 activation, the insulin receptor was still able to activate PI3K.

DISCUSSION

In the current study, we have cloned and expressed the cytoplasmic domain of the retinal insulin receptor, which is functional as demonstrated by its interaction with the p85 subunit of PI3K by two-hybrid assays. Our demonstration that the wild-type receptor hybrids retain the ability to autophosphorylate tyrosine residues shows that the hybrid proteins are properly processed and are enzymatically active in yeast cells. We have also demonstrated that the mutation within the ATP-binding domain in the insulin receptor and

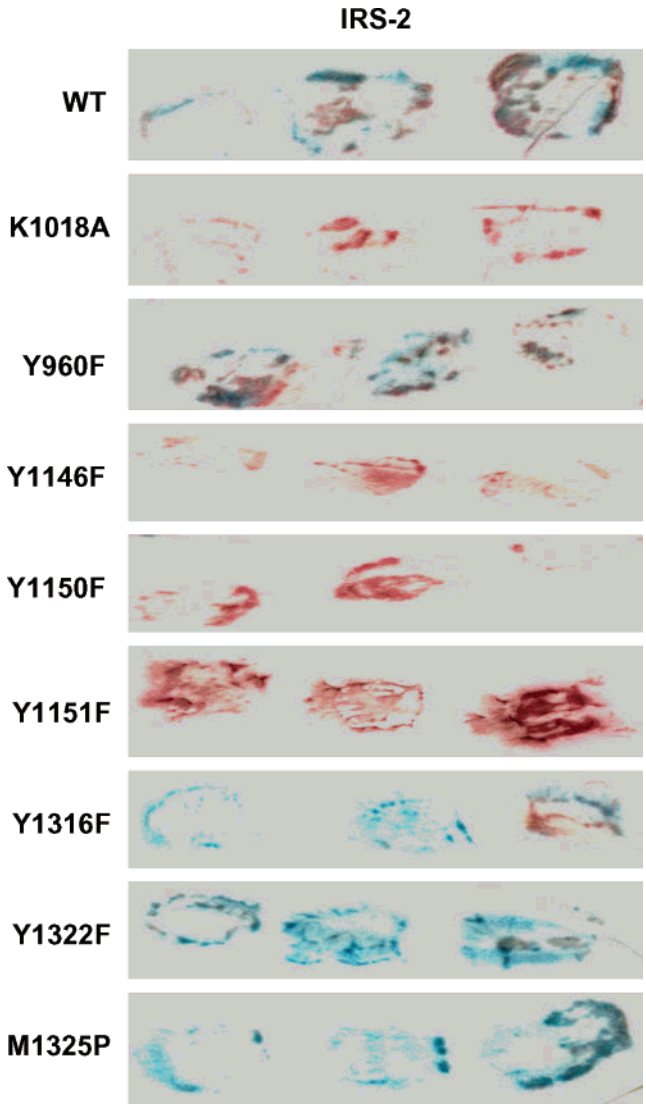

FIGURE 11: Interaction between various mutants of the insulin receptor and a region in IRS-2 containing amino acids 591−786. Yeast two-hybrid assays were carried out between various mutants of the insulin receptor and IRS-2 (amino acids 591−786). Transformants were assayed for β-galactosidase activity for colony color.

mutation in the SH2 domain of the p85 subunit of PI3K clearly establish the absolute requirement of tyrosine kinase activity and SH2-dependent binding between the insulin receptor and p85 subunit of PI3K. Our data also indicate a direct interaction between the insulin receptor and p85 subunit of PI3K. We conclude from these studies that the two-hybrid system accurately reconstitutes the interaction between the receptor and p85 and is thus a valid model for further study.

Recently, we presented evidence that the p85 subunit of PI3K binds directly to the phosphorylated insulin receptor in retina, independent of IRS-1 (*18*). This observation led to the speculation that perhaps IRS-1 and p85 could have a common binding site(s) on IRβ. It has been shown that tyrosine 960 within the insulin receptor juxtamembrane domain is essential for IRS-1 interaction (*44*). Mutation of tyrosine 960 to phenylalanine in the insulin receptor eliminates IRS-1 interaction (*44*, *60*). Further, it has also been shown that the kinase-inactive insulin receptor fails to interact with IRS-1 (*44*). In our yeast two-hybrid assays, mutation

of Y960F completely abolished the binding of IRS-1. However, this mutation did not affect the binding of p85, suggesting that the binding of p85 could be independent of IRS-1.

Our yeast three-hybrid assay also indicated that the interaction between p85 and Y1322-IRβ is dependent on tyrosine kinase activity. This phosphorylated tyrosine moiety failed to interact with IRS-1. Recently, we reported the insulin-independent and light-dependent activation of IRβ in rod photoreceptor cells (*16*) and hypothesized that the phosphorylation of IRβ could be due to the activation of a nonreceptor tyrosine kinase in response to light. It has been shown that cSrc associates with light-activated opsin (*61*), so it may be possible that specific phosphorylation of this tyrosine residue in IRβ by nonreceptor tyrosine kinase could activate a downstream signaling cascade. Consistent with this hypothesis, we have also reported the retinal IRβ phosphorylation by cSrc (*16*). Very recently, we have also reported the phosphorylation of IRβ in response to 17β-estradiol, suggesting that IRβ could be activated other than by insulin; however, the effect is indirect in the activation of IRβ (*62*).

It is interesting to note in this study that neither N-SH2 nor C-SH2 domains of p85 interacted with IRβ (1293−1343) in the three-hybrid assay, although the full-length p85 did interact. On the other hand, wild-type IRβ (amino acids 941−1343) interacted with both full-length and isolated N-SH2 and C-SH2 domains of p85. These results suggest that, for efficient binding between phosphotyrosine and the SH2 domain, the IRβ should be longer in length than the p85 or vice versa. Consistent with this hypothesis, we have previously demonstrated the binding of phosphorylated IRβ (amino acids 1243−1343) to p85 in bovine ROS in vitro (*18*). A weak interaction has also been shown between the isolated domain of Grb10 (SH2) and phosphopeptide Tyr(P)1322 (HIP$_P$YTHMNGG) (*63*). Thus, IRβ and p85 interaction involves more than a simple association between the N-SH2 domain of p85 and the pY1322 residue of IRβ.

Methionine is invariably found in the +3 position of known PI3K binding sites on receptors (*53*). To test the possibility that residues C-terminal to the phosphotyrosine provide specificity for binding to the SH2 domain of IRβ, we changed the +3 position relative to phosphotyrosine to a proline. Substitution of methionine 1325 with proline in our study completely eliminated the interaction between p85 and IRβ. It has been shown previously that the wild-type (Y^{1021}IIP) PDGFR tail does not bind p85; however, substitution of proline with methionine resulted in p85 binding (*64*). In our study, substitution of either Y1322F or M1325P in IRβ resulted in the loss of interaction with p85. These experiments further confirm that Y1322 is the binding site for p85 on IRβ. It is interesting to note that the C-SH2 domain of PLCγ1 interacted with insulin-stimulated IRβ, suggesting that PLCγ1 activity may be regulated through IRβ in the retina. Further detailed studies, however, are required to establish this fact.

There is widespread expression of IRS-1 throughout the retina, and IRS-1 is found in regions of the retina abundant in insulin receptors, including outer segments (*20*). However, in our study, insulin-stimulated IRβ in organ cultures associated with PI3K, independent of IRS-1. We did not find IRS-1 phosphorylation in response to insulin, under conditions that led to the activation of Akt. This observation is in agreement with the recent report that, in an ex vivo system, retinal IRS-1 is not phosphorylated in response to insulin stimulus (*13*). Very recently, IRS-2 was shown to be tyrosine phosphorylated in response to insulin in the retina (*13*). In this study, we have demonstrated the insulin-induced tyrosine-phosphorylated IRS-2 is able to interact with the p85 subunit of PI3K, suggesting that IRS-2 could be involved in the activation of PI 3K. Also, insulin-induced activation of Akt was completely inhibited by the PI3K inhibitor LY294002, suggesting that insulin receptor/PI3K/Akt signaling is operative in the retina independent of IRS-1 but could be dependent on IRS-2.

IRS-1 and IRS-2 have two conserved domains at the NH_2 terminus, called IHI^{PH} and IH2^{PTB}, which resemble a pleckstrin homology (PH) domain and a phosphotyrosine binding (PTB) domain, respectively (*59*, *65*). The IH2^{PTB} domain of IRS-1 and IRS-2 binds to the phosphorylated NPXY motif (Y960) in the IRβ (*59*). IRS-2 interacts with IRβ via a second domain (absent in IRS-1) comprising amino acids 591−786, does not require the NPXY motif, but associates with the catalytic domain of IR containing Y1146, Y1150, and Y1151 residues (*59*).

It is interesting to note in this study that the Y960F mutant insulin receptor is capable of bringing down the p85 subunit of PI3K from retinal lysates. Substitution of Y960F completely abolished the binding mediated through the PTB binding domain of IRS-1 and IRS-2 (*59*). IRS-2 can still interact through a domain between amino acids 591−786 with Y1146, Y1150, and Y1151 residues in the IRβ and activate PI3K. Under our experimental conditions (presence of 4 mM EDTA in the retinal homogenates) the endogenous IRS-2 should not be tyrosine phosphorylated by the mutant Y960F insulin receptor. However, the Y960F mutant insulin receptor is capable of bringing down endogenous p85. Thus, in the absence of IRS-2 activation, the mutant insulin receptor was still able to activate PI3K. These results suggest the existence of multiple pathways in the activation of PI3K in the retina.

IRS-1 is not an exclusive substrate of the insulin receptor but is also a substrate for IGF1 receptors (*66*). In the central nervous system, IRS-1 is present in some regions where there are no insulin and IGF1 receptors (*67*). The IRS proteins are a growing family that are phosphorylated by the activated insulin and IGF-1 receptors, as well as by growth hormone and cytokine receptors (*58*, *68*). It has been shown recently that, in response to insulin and IGF-1, brown preadipocytes derived from IRS-1 knockout animals have an increased apoptotic phenotype involving caspase-3, cAMP response element binding protein, and FKHR (*69*). Inhibition of apoptosis has been observed by reconstitution of IRS proteins (*69*). These results suggest the unique role of IRS proteins in several signaling pathways, at least in the rod outer segments. In retina, IRS-1 has been shown to be widely expressed (*20*), although we have no evidence that it plays a role in the PI3K pathway. Many degenerative diseases show an early loss of rod cells followed by loss of cone cells (*70*), and apoptosis has been shown to be the major pathological phenotype (*71*). Whether IRS family members have any role in these retinal diseases needs to be studied.

ACKNOWLEDGMENT

The technical assistance of Mr. Niket Muni is highly appreciated.

REFERENCES

1. Williams, L. T. (1989) Signal transduction by the platelet-derived growth factor receptor, *Science 243*, 1564−1570.
2. Ullrich, A., and Schlessinger, J. (1990) Signal transduction by receptors with tyrosine kinase activity, *Cell 61*, 203−212.
3. Otsu, M., Hiles, I., Gout, I., Fry, M. J., Ruiz-Larrea, F., Panayotou, G., Thompson, A., Dhand, R., Hsuan, J., and Totty, N. (1991) Characterization of two 85 kd proteins that associate with receptor tyrosine kinases, middle-T/pp60c-src complexes, and PI3-kinase, *Cell 65*, 91−104.
4. Skolnik, E. Y., Margolis, B., Mohammadi, M., Lowenstein, E., Fischer, R., Drepps, A., Ullrich, A., and Schlessinger, J. (1991) Cloning of PI3 kinase-associated p85 utilizing a novel method for expression/cloning of target proteins for receptor tyrosine kinases, *Cell 65*, 83−90.
5. Hu, P., Mondino, A., Skolnik, E. Y., and Schlessinger, J. (1993) Cloning of a novel, ubiquitously expressed human phosphatidylinositol 3-kinase and identification of its binding site on p85, *Mol. Cell. Biol. 13*, 7677−7688.
6. Klippel, A., Escobedo, J. A., Fantl, W. J., and Williams, L. T. (1992) The C-terminal SH2 domain of p85 accounts for the high affinity and specificity of the binding of phosphatidylinositol 3-kinase to phosphorylated platelet-derived growth factor beta receptor, *Mol. Cell. Biol. 12*, 1451−1459.
7. White, M. F., and Kahn, C. R. (1994) The insulin signaling system, *J. Biol. Chem. 269*, 1−4.
8. DeFronzo, R. A., Bonadonna, R. C., and Ferrannini, E. (1992) Pathogenesis of NIDDM. A balanced overview, *Diabetes Care 15*, 318−368.
9. Van Horn, D. J., Myers, M. G., Jr., and Backer, J. M. (1994) Direct activation of the phosphatidylinositol 3′-kinase by the insulin receptor, *J. Biol. Chem. 269*, 29−32.
10. Backer, J. M., Myers, M. G., Jr., Shoelson, S. E., Chin, D. J., Sun, X. J., Miralpeix, M., Hu, P., Margolis, B., Skolnik, E. Y., and Schlessinger, J. (1992) Phosphatidylinositol 3′-kinase is activated by association with IRS-1 during insulin stimulation, *EMBO J. 11*, 3469−3479.
11. Havrankova, J., Roth, J., and Brownstein, M. (1978) Insulin receptors are widely distributed in the central nervous system of the rat, *Nature 272*, 827−829.
12. Waldbillig, R. J., Fletcher, R. T., Chader, G. J., Rajagopalan, S., Rodrigues, M., and LeRoith, D. (1987) Retinal insulin receptors. 1. Structural heterogeneity and functional characterization, *Exp. Eye Res. 45*, 823−835.
13. Reiter, C. E., Sandirasegarane, L., Wolpert, E. B., Klinger, M., Simpson, I. A., Barber, A. J., Antonetti, D. A., Kester, M., and Gardner, T. W. (2003) Characterization of insulin signaling in rat retina in vivo and ex vivo, *Am. J. Physiol. 285*, E763−E774.
14. Reiter, C. E., and Gardner, T. W. (2003) Functions of insulin and insulin receptor signaling in retina: possible implications for diabetic retinopathy, *Prog. Retinal Eye Res. 22*, 545−562.
15. Rodrigues, M., Waldbillig, R. J., Rajagopalan, S., Hackett, J., LeRoith, D., and Chader, G. J. (1988) Retinal insulin receptors: localization using a polyclonal anti-insulin receptor antibody, *Brain Res. 443*, 389−394.
16. Rajala, R. V., McClellan, M. E., Ash, J. D., and Anderson, R. E. (2002) In vivo regulation of phosphoinositide 3-kinase in retina through light-induced tyrosine phosphorylation of the insulin receptor beta-subunit, *J. Biol. Chem. 277*, 43319−43326.
17. Guo, X., Ghalayini, A. J., Chen, H., and Anderson, R. E. (1997) Phosphatidylinositol 3-kinase in bovine photoreceptor rod outer segments, *Invest. Ophthalmol. Visual Sci. 38*, 1873−1882.
18. Rajala, R. V., and Anderson, R. E. (2001) Interaction of the insulin receptor beta-subunit with phosphatidylinositol 3-kinase in bovine ROS, *Invest. Ophthalmol. Visual Sci. 42*, 3110−3117.
19. Rajala, R. V., and Anderson, R. E. (2003) Light regulation of the insulin receptor in the retina, *Mol. Neurobiol. 28*, 128−138.
20. Gosbell, A. D., Favilla, I., Baxter, K. M., and Jablonski, P. (2000) Insulin receptor and insulin receptor substrate-I in rat retinae, *Clin. Exp. Ophthalmol. 28*, 212−215.
21. White, M. F., Livingston, J. N., Backer, J. M., Lauris, V., Dull, T. J., Ullrich, A., and Kahn, C. R. (1988) Mutation of the insulin receptor at tyrosine 960 inhibits signal transmission but does not affect its tyrosine kinase activity, *Cell 54*, 641−649.
22. Kapeller, R., Chen, K. S., Yoakim, M., Schaffhausen, B. S., Backer, J., White, M. F., Cantley, L. C., and Ruderman, N. B. (1991) Mutations in the juxtamembrane region of the insulin receptor impair activation of phosphatidylinositol 3-kinase by insulin, *Mol. Endocrinol. 5*, 769−777.
23. Araki, E., Lipes, M. A., Patti, M. E., Bruning, J. C., Haag, B., III, Johnson, R. S., and Kahn, C. R. (1994) Alternative pathway of insulin signalling in mice with targeted disruption of the IRS-1 gene, *Nature 372*, 186−190.
24. Tamemoto, H., Kadowaki, T., Tobe, K., Yagi, T., Sakura, H., Hayakawa, T., Terauchi, Y., Ueki, K., Kaburagi, Y., Satoh, S., Sekihara, H., Yoshioka, S., Horikoshi, H., Furuta, Y., Ikawa, Y., Kasuga, M., Yazaki, Y., and Aizawa, S. (1994) Insulin resistance and growth retardation in mice lacking insulin receptor substrate-1, *Nature 372*, 182−186.
25. Kelly, K. L., Ruderman, N. B., and Chen, K. S. (1992) Phosphatidylinositol-3-kinase in isolated rat adipocytes. Activation by insulin and subcellular distribution, *J. Biol. Chem. 267*, 3423−3428.
26. Kelly, K. L., and Ruderman, N. B. (1993) Insulin-stimulated phosphatidylinositol 3-kinase. Association with a 185-kDa tyrosine-phosphorylated protein (IRS-1) and localization in a low-density membrane vesicle, *J. Biol. Chem. 268*, 4391−4398.
27. Shao, J., Yamashita, H., Qiao, L., Draznin, B., and Friedman, J. E. (2002) Phosphatidylinositol 3-kinase redistribution is associated with skeletal muscle insulin resistance in gestational diabetes mellitus, *Diabetes 51*, 19−29.
28. Goldstein, B. J., and Dudley, A. L. (1990) The rat insulin receptor: primary structure and conservation of tissue-specific alternative messenger RNA splicing, *Mol. Endocrinol. 4*, 235−244.
29. He, W., Rose, D. W., Olefsky, J. M., and Gustafson, T. A. (1998) Grb10 interacts differentially with the insulin receptor, insulin-like growth factor I receptor, and epidermal growth factor receptor via the Grb10 Src homology 2 (SH2) domain and a second novel domain located between the pleckstrin homology and SH2 domains, *J. Biol. Chem. 273*, 6860−6867.
30. Tsiokas, L., Kim, E., Arnould, T., Sukhatme, V. P., and Walz, G. (1997) Homo- and heterodimeric interactions between the gene products of PKD1 and PKD2, *Proc. Natl. Acad. Sci. U.S.A. 94*, 6965−6970.
31. Vojtek, A. B., Hollenberg, S. M., and Cooper, J. A. (1993) Mammalian Ras interacts directly with the serine/threonine kinase Raf, *Cell 74*, 205−214.
32. Breeden, L., and Nasmyth, K. (1985) Regulation of the yeast HO gene, *Cold Spring Harbor Symp. Quant. Biol. 50*, 643−650.
33. Tsiokas, L., Arnould, T., Zhu, C., Kim, E., Walz, G., and Sukhatme, V. P. (1999) Specific association of the gene product of PKD2 with the TRPC1 channel, *Proc. Natl. Acad. Sci. U.S.A. 96*, 3934−3939.
34. Bendixen, C., Gangloff, S., and Rothstein, R. (1994) A yeast mating-selection scheme for detection of protein−protein interactions, *Nucleic Acids Res. 22*, 1778−1779.
35. Breeden, L., and Nasmyth, K. (1987) Cell cycle control of the yeast HO gene: cis- and trans-acting regulators, *Cell 48*, 389−397.
36. Lioubin, M. N., Algate, P. A., Tsai, S., Carlberg, K., Aebersold, A., and Rohrschneider, L. R. (1996) p150Ship, a signal transduction molecule with inositol polyphosphate-5-phosphatase activity, *Genes Dev. 10*, 1084−1095.
37. Keegan, K., and Cooper, J. A. (1996) Use of the two hybrid system to detect the association of the protein-tyrosine-phosphatase, SHPTP2, with another SH2-containing protein, Grb7, *Oncogene 12*, 1537−1544.
38. Olson, A. L., Eyster, C. A., Duggins, Q. S., and Knight, J. B. (2003) Insulin promotes formation of polymerized microtubules by a phosphatidylinositol 3-kinase-independent, actin-dependent pathway in 3T3-L1 adipocytes, *Endocrinology 144*, 5030−5039.
39. Kaplan, D. R., Whitman, M., Schaffhausen, B., Pallas, D. C., White, M., Cantley, L., and Roberts, T. M. (1987) Common elements in growth factor stimulation and oncogenic transformation: 85 kd phosphoprotein and phosphatidylinositol kinase activity, *Cell 50*, 1021−1029.
40. McGlade, C. J., Ellis, C., Reedijk, M., Anderson, D., Reith, A. D., Panayotou, G., End, P., Bernstein, A., Kazlauskas, A., Waterfield, M. D., and Pawson, T. (1992) SH2 domains of the

p85 alpha subunit of phosphatidylinositol 3-kinase regulate binding to growth factor receptors, *Mol. Cell. Biol. 12*, 991−997.
41. Araki, E., Sun, X. J., Haag, B. L., III, Chuang, L. M., Zhang, Y., Yang-Feng, T. L., White, M. F., and Kahn, C. R. (1993) Human skeletal muscle insulin receptor substrate-1. Characterization of the cDNA, gene, and chromosomal localization, *Diabetes 42*, 1041−1054.
42. Backer, J. M., Myers, M. G., Jr., Sun, X. J., Chin, D. J., Shoelson, S. E., Miralpeix, M., and White, M. F. (1993) Association of IRS-1 with the insulin receptor and the phosphatidylinositol 3′-kinase. Formation of binary and ternary signaling complexes in intact cells, *J. Biol. Chem. 268*, 8204−8212.
43. Ullrich, A., Bell, J. R., Chen, E. Y., Herrera, R., Petruzzelli, L. M., Dull, T. J., Gray, A., Coussens, L., Liao, Y. C., Tsubokawa, M., Mason, A., Seeburg, P. H., Grunfeld, C., Rosen, O. M., and Ramachandran, J. (1985) Human insulin receptor and its relationship to the tyrosine kinase family of oncogenes, *Nature 313*, 756−761.
44. O'Neill, T. J., Craparo, A., and Gustafson, T. A. (1994) Characterization of an interaction between insulin receptor substrate 1 and the insulin receptor by using the two-hybrid system, *Mol. Cell. Biol. 14*, 6433−6442.
45. Ebina, Y., Ellis, L., Jarnagin, K., Edery, M., Graf, L., Clauser, E., Ou, J. H., Masiarz, F., Kan, Y. W., Goldfine, I. D., Roth, R. A., and Rutter, W. J. (1985) The human insulin receptor cDNA: the structural basis for hormone-activated transmembrane signalling, *Cell 40*, 747−758.
46. Sternberg, M. J., and Taylor, W. R. (1984) Modelling the ATP-binding site of oncogene products, the epidermal growth factor receptor and related proteins, *FEBS Lett. 175*, 387−392.
47. Chou, C. K., Dull, T. J., Russell, D. S., Gherzi, R., Lebwohl, D., Ullrich, A., and Rosen, O. M. (1987) Human insulin receptors mutated at the ATP-binding site lack protein tyrosine kinase activity and fail to mediate postreceptor effects of insulin, *J. Biol. Chem. 262*, 1842−1847.
48. Ebina, Y., Araki, E., Taira, M., Shimada, F., Mori, M., Craik, C. S., Siddle, K., Pierce, S. B., Roth, R. A., and Rutter, W. J. (1987) Replacement of lysine residue 1030 in the putative ATP-binding region of the insulin receptor abolishes insulin- and antibody-stimulated glucose uptake and receptor kinase activity, *Proc. Natl. Acad. Sci. U.S.A. 84*, 704−708.
49. McClain, D. A., Maegawa, H., Lee, J., Dull, T. J., Ulrich, A., and Olefsky, J. M. (1987) A mutant insulin receptor with defective tyrosine kinase displays no biologic activity and does not undergo endocytosis, *J. Biol. Chem. 262*, 14663−14671.
50. Blom, N., Gammeltoft, S., and Brunak, S. (1999) Sequence and structure-based prediction of eukaryotic protein phosphorylation sites, *J. Mol. Biol. 294*, 1351−1362.
51. Rajala, R. V., Datla, R. S., Carlsen, S. A., Anderson, D. H., Qi, Z., Wang, J. H., and Sharma, R. K. (2001) Phosphorylation of human N-myristoyltransferase by N-myristoylated SRC family tyrosine kinase members, *Biochem. Biophys. Res. Commun. 288*, 233−239.
52. Staubs, P. A., Reichart, D. R., Saltiel, A. R., Milarski, K. L., Maegawa, H., Berhanu, P., Olefsky, J. M., and Seely, B. L. (1994) Localization of the insulin receptor binding sites for the SH2 domain proteins p85, Syp, and GAP, *J. Biol. Chem. 269*, 27186−27192.
53. Cantley, L. C., Auger, K. R., Carpenter, C., Duckworth, B., Graziani, A., Kapeller, R., and Soltoff, S. (1991) Oncogenes and signal transduction, *Cell 64*, 281−302.
54. Songyang, Z., Shoelson, S. E., Chaudhuri, M., Gish, G., Pawson, T., Haser, W. G., King, F., Roberts, T., Ratnofsky, S., Lechleider, R. J., Neel, B. G., Birge, R. B., Fajardo, J. E., Chou, M. M., Hanafusa, H., Schaffhausen, B., and Cantley, L. C. (1993) SH2 domains recognize specific phosphopeptide sequences, *Cell 72*, 767−778.
55. Ruderman, N. B., Kapeller, R., White, M. F., and Cantley, L. C. (1990) Activation of phosphatidylinositol 3-kinase by insulin, *Proc. Natl. Acad. Sci. U.S.A. 87*, 1411−1415.
56. Ghalayini, A. J., Weber, N. R., Rundle, D. R., Koutz, C. A., Lambert, D., Guo, X. X., and Anderson, R. E. (1998) Phospholipase Cgamma1 in bovine rod outer segments: immunolocalization and light-dependent binding to membranes, *J. Neurochem. 70*, 171−178.
57. Bell, M. W., Alvarez, K., and Ghalayini, A. J. (1999) Association of the tyrosine phosphatase SHP-2 with transducin-alpha and a 97-kDa tyrosine-phosphorylated protein in photoreceptor rod outer segments, *J. Neurochem. 73*, 2331−2340.
58. White, M. F. (1997) The insulin signaling system and the IRS proteins, *Diabetologia 40* (Suppl. 2), S2−S17.
59. Sawka-Verhelle, D., Tartare-Deckert, S., White, M. F., and Van Obberghen, E. (1996) Insulin receptor substrate-2 binds to the insulin receptor through its phosphotyrosine-binding domain and through a newly identified domain comprising amino acids 591−786, *J. Biol. Chem. 271*, 5980−5983.
60. Gustafson, T. A., He, W., Craparo, A., Schaub, C. D., and O'Neill, T. J. (1995) Phosphotyrosine-dependent interaction of SHC and insulin receptor substrate 1 with the NPEY motif of the insulin receptor via a novel non-SH2 domain, *Mol. Cell. Biol. 15*, 2500−2508.
61. Ghalayini, A. J., Desai, N., Smith, K. R., Holbrook, R. M., Elliott, M. H., and Kawakatsu, H. (2002) Light-dependent association of Src with photoreceptor rod outer segment membrane proteins in vivo, *J. Biol. Chem. 277*, 1469−1476.
62. Yu, X., Rajala, R. V., McGinnis, J. F., Li, F., Anderson, R. E., Yan, X., Li, S., Elias, R. V., Knapp, R. R., and Cao, W. (2004) Involvement of insulin/PI3K/Akt signal pathway in 17beta-estradiol-mediated neuroprotection, *J. Biol. Chem. 279*, 13086−13094.
63. Hansen, H., Svensson, U., Zhu, J., Laviola, L., Giorgino, F., Wolf, G., Smith, R. J., and Riedel, H. (1996) Interaction between the Grb10 SH2 domain and the insulin receptor carboxyl terminus, *J. Biol. Chem. 271*, 8882−8886.
64. Larose, L., Gish, G., Shoelson, S., and Pawson, T. (1993) Identification of residues in the beta platelet-derived growth factor receptor that confer specificity for binding to phospholipase C-gamma 1, *Oncogene 8*, 2493−2499.
65. White, M. F. (1998) The IRS-signalling system: a network of docking proteins that mediate insulin action, *Mol. Cell. Biochem. 182*, 3−11.
66. Myers, M. G., Jr., Sun, X. J., Cheatham, B., Jachna, B. R., Glasheen, E. M., Backer, J. M., and White, M. F. (1993) IRS-1 is a common element in insulin and insulin-like growth factor-I signaling to the phosphatidylinositol 3′-kinase, *Endocrinology 132*, 1421−1430.
67. Folli, F., Bonfanti, L., Renard, E., Kahn, C. R., and Merighi, A. (1994) Insulin receptor substrate-1 (IRS-1) distribution in the rat central nervous system, *J. Neurosci. 14*, 6412−6422.
68. Yenush, L., and White, M. F. (1997) The IRS-signalling system during insulin and cytokine action, *BioEssays 19*, 491−500.
69. Tseng, Y. H., Ueki, K., Kriauciunas, K. M., and Kahn, C. R. (2002) Differential roles of insulin receptor substrates in the anti-apoptotic function of insulin-like growth factor-1 and insulin, *J. Biol. Chem. 277*, 31601−31611.
70. Schmidt, S. Y. (1985) *Handbook of Neurochemistry*, Plenum, New York.
71. Alfinito, P. D., and Townes-Anderson, E. (2002) Activation of mislocalized opsin kills rod cells: a novel mechanism for rod cell death in retinal disease, *Proc. Natl. Acad. Sci. U.S.A. 99*, 5655−5660.

BI035913V